Materials Transactions, Vol. 55, No. 1 (2014) pp. 13 to 18
Special Issue on Strength of Fine Grained Materials — 60 Years of Hall–Petch —

OVERVIEW

Superior Strength in Ultrafine-Grained Materials Produced by SPD Processing

Ruslan Z. Valiev[1,2]

[1]*Institute of Physics of Advanced Materials, Ufa State Aviation Technical University, 12 K. Marx. Str., Ufa 450000, Russia*
[2]*Laboratory for Mechanics of Bulk Nanomaterials, Saint Petersburg State University, Universitetsky prospekt, 28, Peterhof, 198504, Saint Petersburg, Russia*

Recent studies demonstrated that the processing of metallic alloys by severe plastic deformation (SPD) can result in not only strong grain refinement but also leads to the formation of grain boundaries (GBs) with different structures, including GB segregations and precipitations. These nanostructural features of SPD-processed alloys produce considerable influence on their mechanical properties. The paper presents experimental data demonstrating a superstrength and "positive" slope of the Hall–Petch relation when passing from micro- to nanostructured state in a number of metallic materials subjected to severe plastic deformation. The nature of the superior strength is associated with new strengthening mechanisms and the difficulty of generation of dislocations from grain boundaries with segregations.

This new approach is used for achieving the enhanced strength in several commercial Al and Ti alloys as well as steels subjected to SPD processing. [doi:10.2320/matertrans.MA201325]

(Received September 4, 2013; Accepted October 16, 2013; Published December 25, 2013)

Keywords: *The Hall–Petch relation, severe plastic deformation (SPD), superstrength, nanostructured metals and alloys*

1. Introduction

Although the mechanical and physical properties of all crystalline materials are determined by several microstructural parameters, the average grain size of the material generally plays a very significant, and often a dominant role. It is well known that the strength of polycrystalline materials is typically related to the grain size, d, through the Hall–Petch (H–P) equation which states that the yield stress, σ_y, is given by

$$\sigma_y = \sigma_0 + k_y d^{-1/2} \quad (1)$$

where σ_0 is termed the friction stress and k_y is a constant of yielding.[1,2] It follows from eq. (1) that the strength increases with a reduction in the grain size and this has led to an ever-increasing interest in fabricating materials with extremely small grain sizes.

During last two decades severe plastic deformation (SPD) processing has attracted significant research interest because it is an effective way to produce ultrafine-grained (UFG) metals and alloys — that results in the enhancement of various mechanical and functional properties.[3,4] Fabrication of UFG materials has a special interest for fundamental studies of the H–P-relation, since there are various "anomalies" in the H–P behaviour for materials with ultrafine grains. Thus for nanosized grains (20–50 nm) the relation is reported to be violated so that the H–P plot deviates from linear dependence at lower stress values and its slope k_y often becomes negative.[5,6] That is associated with the changes in the deformation mechanisms for ultrafine-grained sizes. In recent years this problem has been widely analyzed in both experimental and theoretical studies.[7,8] At the same time in the ultrafine-grained materials with the size of 100–200 nm produced by SPD processing, we observed "positive" slope of the H–P relation[9,10] when UFG alloys can exhibit a considerably higher strength than the H–P relationship predicts for the range of ultrafine grains.

Here we should highlight one important feature of the H–P equation by formula (1) that it doesn't explicitly consider parameters of the grain boundaries structures. At the same time the critical parameter for UFG metals and alloys produced by severe plastic deformation together with the refinement of microstructure to the nano-sized range is the grain boundary structure because the boundaries can be formed as low- and high-angle, special and random, equilibrium and non-equilibrium boundaries with dislocation arrays, but it depends on the SPD processing regimes.[3,11] Furthermore, boundaries having different structures exhibit different transport mechanisms (deformation, diffusion, etc.), e.g., grain boundary sliding which in turn leads to differences in the properties. This opens a new way for advancing the properties of ultrafine-grained materials by appropriately tuning their grain boundary structures.

In recent years in our laboratory in close collaboration with colleagues and partners there were performed a number of investigations of unusual mechanical performance of SPD-processed Al and Ti alloys as well as in several steels.[9,12–16] In continuation of these works the present study deals with consideration and investigation of manifestation and nature of superstrength, which was observed in several nanostructured materials.

2. Experimental

The objects of this research were several pure metals as well as commercial Al–Mg–Si alloys, austenitic steel and low carbon steels. In order to obtain an UFG structure, the solid-solute alloys were subjected to high-pressure torsion (HPT) and equal channel angular pressing (ECAP). For HPT-processing the applied pressure of 6 GPa and 20 rotations were used to process the alloys. The produced samples had the form of discs with a diameter of 20 and 0.6 mm in thickness, which are well suited for mechanical tests. ECAP processing has been performed with the dies of 10 and 20 mm in diameter.[17]

The structural characterization was performed by transmission electron microscopy (TEM), X-ray diffraction (XRD) and atom probe tomography (APT). A mean grain

size and a grain size distribution were estimated from TEM dark-field measurements in torsion plane over more than 350 grains from an area situated at the middle of an HPT disc radius. Selected-area electron diffraction (SAED) patterns have been taken from the area of 1.3 μm in diameter. XRD was performed with a Pan Analytical X'Pert diffractometer using Cu Ka radiation (50 kV and 40 mA). The lattice parameter a for the initial and HPT-processed alloys was calculated from X-ray data according to the Nelson–Riley extrapolation method.[18] Tensile tests have been precisely performed using a laser extensometer at room temperature with a strain rate of $10^{-4}\,s^{-1}$ on a computer-controlled testing machine operating with a constant displacement of the specimen grips. Strength characteristics were estimated by testing samples with a gage of $2.0 \times 1.0 \times 0.4\,mm^3$.

3. Results and Discussions

3.1 Grain boundaries in SPD-processed materials

Although it is possible to achieve a nanocrystalline structure with a grain size less than 100 nm in a number of metals and alloys by means of HPT,[19,20] for SPD processing by ECAP and HPT it is typical to form ultrafine-grained structures with mean grain sizes within the submicrometer range so that, usually, the grain sizes are ~100–300 nm.[17] At the same time depending on the SPD processing regimes (amount of strain, temperature and strain rate, applied pressure) the formation of various grain boundaries takes place as well so that excess dislocations, twins, grain boundary segregations and precipitations also can introduce a considerable influence on the properties of UFG materials after processing.

In general, in our studies four types of grain boundaries have been identified in UFG metals and alloys produced by SPD that can be observed through the application of modern techniques of structural analysis such as high-resolution transmission electron microscopy (HRTEM), 3D-atom probe, etc.[3,4,9,11–15,19] These GB types are as follows.

3.1.1 Low-angle and high angle GBs

It was shown already in the earlier studies of nano SPD materials that processing with true accumulative strains $\varepsilon > 6$–8 leads to the formation of ultrafine grains with mostly high angle GBs.[19] This conclusion was confirmed by observations of superplasticity in these UFG metals, because its basic mechanism, namely, GB sliding can take place only along high angle boundaries.

Many subsequent experiments conducted using the electron backscattered diffraction (EBSD) analysis provided direct evidence that the cell and subgrain structures with low-angle boundaries, formed at the early stages of SPD processing, continuously transform into UFG structures with predominantly high-angle grain boundaries during further processing.[17,20] Such transformations were observed in different metals and alloys during HPT, ECAP and other techniques of SPD processing.

3.1.2 Special and random GBs

Special twin boundaries were observed in many UFG materials, processed by SPD. For example, such GBs are typical of the materials after ECAP at lower temperatures and/or those subjected to additional cold rolling, extrusion or drawing. Figure 1 shows a TEM image of atom resolution of UFG Cu after ECAP and cold rolling at liquid nitrogen temperature with clearly observed twins of 10–20 nm in size.[21]

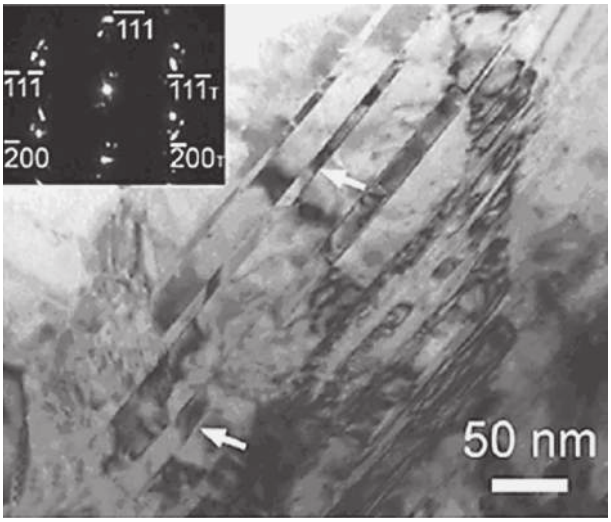

Fig. 1 TEM image of a typical grain with a high density of deformation twins (indicated by arrows) in UFG Cu processed by ECAP with subsequent cold rolling.[21]

Twin boundaries have been also often observed in UFG metals with low stacking fault energy, e.g., in an austenitic stainless steel subjected to SPD processing.[19]

3.1.3 Non-equilibrium GBs with dislocation arrays

They are those possessing the excess energy, long-range stresses, enhanced free volume and their formation typically results from the interaction of lattice dislocation and grain boundaries.[19] For example, as illustrated in Fig. 2[22] an excessively high density of dislocations, facets and steps are observed at grain boundaries of the UFG alloy Al–3% Mg after HPT that led to a non-equilibrium state of boundaries with a crystal lattice distortion zone of ~3–5 nm in width.[19,23] Non-equilibrium grain boundaries with dislocation arrays are typical for different materials after SPD processing and their role in the mechanical behavior of UFG materials has been studied in a number of reports.[19,23,24]

3.1.4 GB segregations and precipitations

Recent investigations with the application of ion microscopy and 3D-atom probe tomography directly testify to the formation of segregations of impurity and alloying elements at grain boundaries in UFG alloys processed by SPD[12,25,26] as shown, for example, in Fig. 3.[12] These segregations form "clouds" or clusters ~3–5 nm in size which can produce influence on the generation and motion of dislocations which accordingly leads to additional strengthening of the alloys.[9,12,25,27]

Thus, various kinds of grain boundaries can exist in UFG metals and alloys, processed by SPD and these GBs features should be considered during their mechanical behaviour analysis.

3.2 Observation of superstrength in UFG metals

As was noticed above, the high strength of SPD-processed materials is usually related to the formation of the UFG structure via the H–P relationship according to the eq. (1).

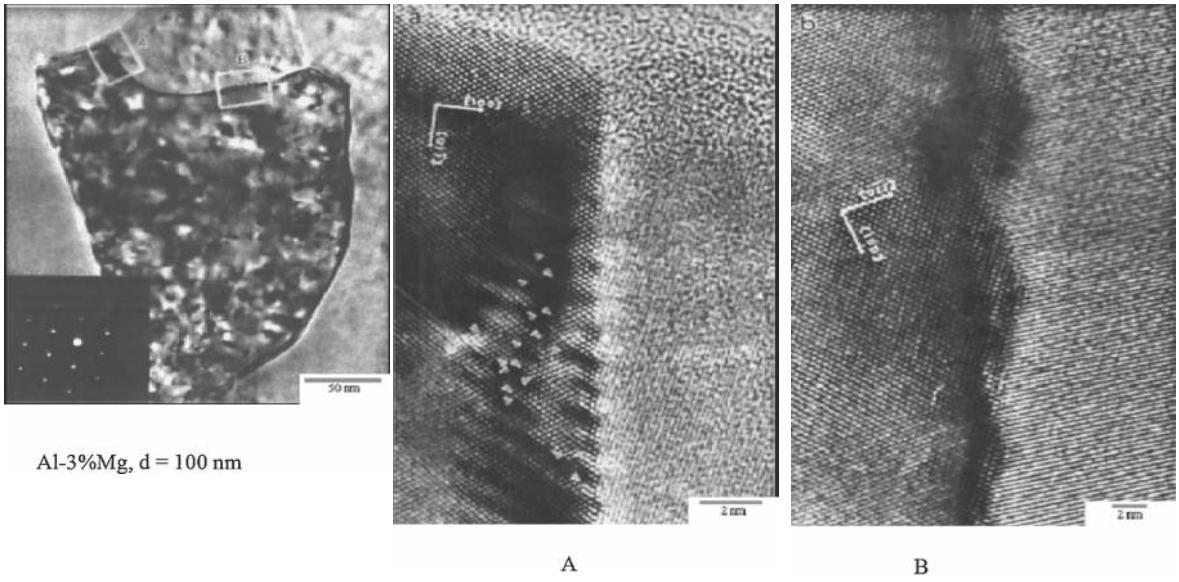

Fig. 2 TEM image of non-equilibrium grain boundaries in the UFG Al–3% Mg alloy with a grain of ~100 nm in size[22] (orientation indexes are given in the low left) illustrating high resolution photographs of regions A and B.

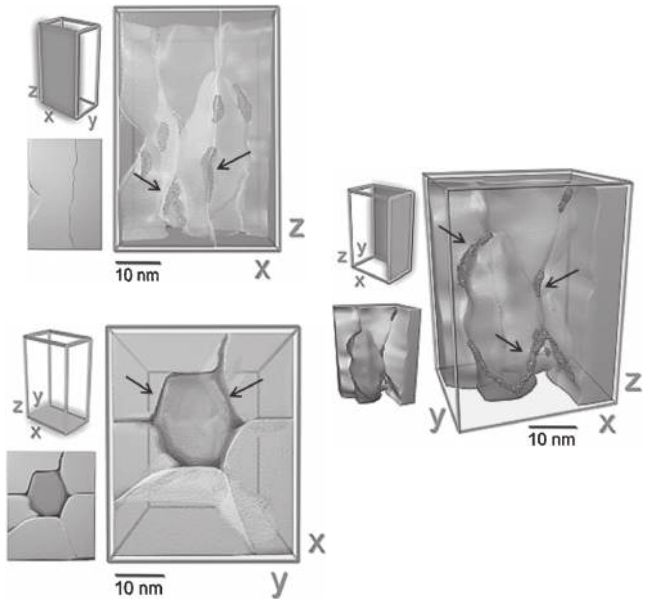

Fig. 3 Tomographic view of the nanostructure of UFG alloy Al-7075. The segregations of alloying elements (indicated by arrows) are observed at grain boundaries and junctions.[12]

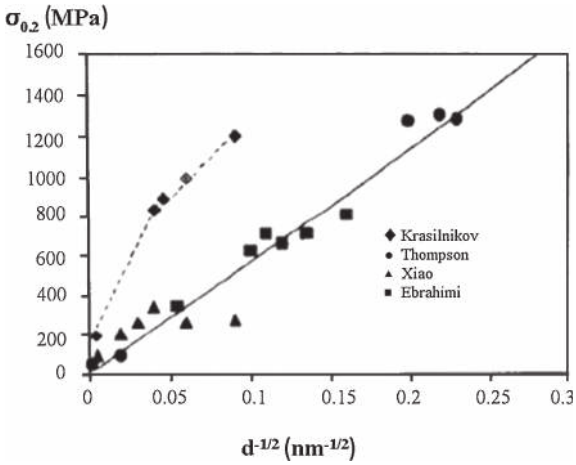

Fig. 4 Yield stress as a function of $d^{-1/2}$ for Ni: the continuous line is for material states with grains without substructure and the dashed line is for UFG Ni containing a dislocation substructure.

However, several our recent studies have shown that the σ_y value in UFG materials processed by SPD may be considerably higher than calculated from the H–P relation.[9,10,13–16,28]

For example, this was revealed in the studies of mechanical behavior of Ni subjected to ECAP and subsequent rolling.[28] Figure 4 shows the difference in strength between the states of Ni where the grains contain dislocation substructures within their interior and where the grains contain no substructure.[29–31] An attempt was made to describe quantitatively the deviation from the H–P rule by taking into account the influence of two types of boundaries, high-angle boundaries (HAB) between grains and low-angle cell boundaries (LAB), on the yield stress of the material. Following an earlier analysis,[32] it was assumed that each of these types of boundaries, and also the nonequilibrium state of grain boundaries, contributes in an independent way to the yield stress:[28]

$$\sigma_y = \sigma_o + \sigma_{LAB} + \sigma_{HAB} + \sigma_{NGBs} \quad (2)$$

and

$$\sigma_y = \sigma_o + M\alpha Gb((1.5S_v\theta/b)_{LAB})^{1/2} + k_y d^{-1/2} + M\alpha Gb(\rho_{GBDs})^{1/2}, \quad (3)$$

where σ_o is the threshold stress, M is the Taylor factor ($M = 3$), α is a constant ($\alpha = 0.24$), G is the shear modulus (79 GPa), b is the Burgers vector (0.249 nm), the term S_v is associated with the cell size, θ is the misorientation angle of the LAB, d is the average grain size, ρ_{GBDs} is the density of extrinsic grain boundary dislocations and k_y is the H–P constant. The numerical values for the constants were taken from the earlier report.[32]

The contributions of these different components for SPD Ni correspond well to the experimentally obtained data as

Table 1 The contribution to flow stress for SPD Ni.

Processing of Ni	YS_{exp}, (Mpa)	YS_{calc}, (Mpa)	σ_{LAB}, (Mpa)	σ_{HAB}, (Mpa)	σ_{GBDs}, (MPa)
ECAP + rolling	990	980	510	280	170
HPT	1200	1190	—	460	710

YS_{exp}–experimental data, YS_{calc}–calculated by means of eq. (3).

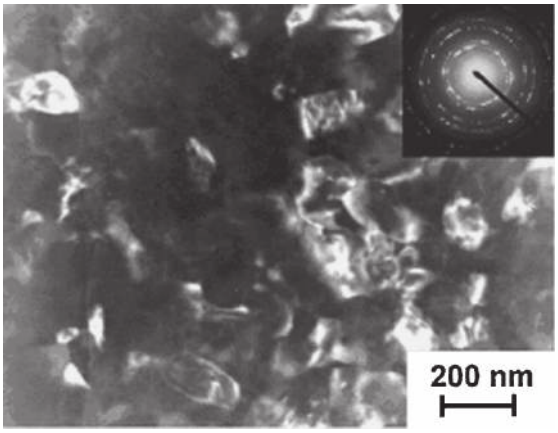

Fig. 5 Typical UFG structure formed in the alloy 1570 after HPT-processing at room temperature (dark field).

shown in Table 1. After HPT a homogeneous UFG structure was formed with mainly high-angle misorientations. Therefore, for the HPT sample it is reasonable to neglect the contribution of low-angle boundaries. Thus, the analysis of mechanical test data shows that the presence of dislocation substructure and the nonequilibrium GB with dislocation arrays contributes more strongly to the yield stress of SPD Ni than the strength calculated according to the H–P rule for a material with the given grain size.

In addition to the dislocation substructure and non-equilibrium grain boundaries, other nanostructured elements as GB segregations and precipitates formed in the UFG materials processed by severe plastic deformation may also contribute to the change of yield stress and flow stress. This issue was recently studied in detail for the case of super-strong UFG Al alloys, namely, Al–Mg, Al 1570 and 7475 alloys.[9,16,27)]

Analysis by TEM demonstrated that HPT leads to a complete transformation of the initial coarse-grained structure of the alloys into the UFG structure. In the alloys 1570 and 7475, homogeneous UFG structures with a grain size of about 100 nm are formed after HPT as shown in Fig. 5. It was also determined that HPT processing has a visible effect on the value of the crystal lattice parameter a of Al alloys. For example, in the 1570 alloy its value after straining was reduced considerably by comparison with the initial state, from 4.0765 ± 0.00001 nm to 4.0692 ± 0.00003 nm which results from the formation of Mg segregations at the grain boundaries.[9,27)]

Figure 6 shows the results of mechanical testing of the 1570 and 7475 alloys. It can be seen that the UFG alloys processed by HPT at room temperature demonstrate record strength that more than twice exceeds the level of strength of the material subjected to standard hardening.

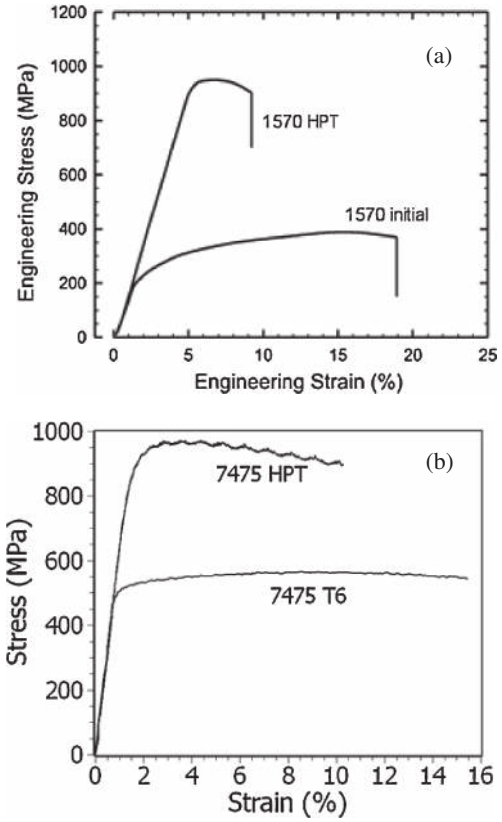

Fig. 6 Engineering stress–strain curves of the UFG alloys Al 1570 (a) and Al 7475 (b) processed by HPT in comparison with standard treatment.

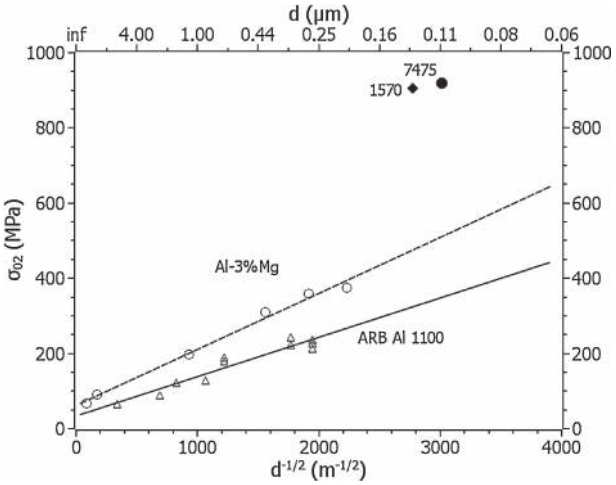

Fig. 7 The H–P relation for the alloys 1100,[33)] Al–3%Mg[34)] and data on the yield stresses of the UFG alloys 1570 and 7475.

Figure 7 shows the data for a number of Al alloys presented in the form of the H–P relation in which the yield stress ($\sigma_{0.2}$) is plotted against the inverse square root of the grain size ($d^{-1/2}$) for a UFG Al alloy 1100 produced by accumulative roll bonding (ARB) and consequent heat treatment[33)] as well as for an ECAP-processed alloy Al–3% Mg alloy.[34)] For the H–P relation in the 1100 alloy,[33)] the following parameters were set: $\sigma_o = 6.0$ MPa and $k_y = 105$ (for the grain sizes in μm); for the ECAP-processed alloy Al–3%Mg,[34)] $\sigma_o = 62$ MPa and $k_y = 149$. Figure 7 also shows the data obtained for the coarse-grained (CG) and UFG 1570 and 7475 alloys.

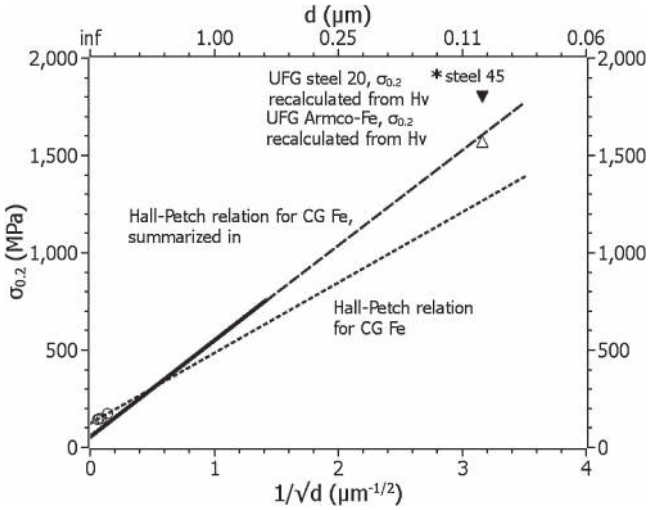

Fig. 8 The H–P relation for Armco-Fe[36] and iron[37] and data on the yield stresses of UFG Fe[39,41] and steel 20.[40]

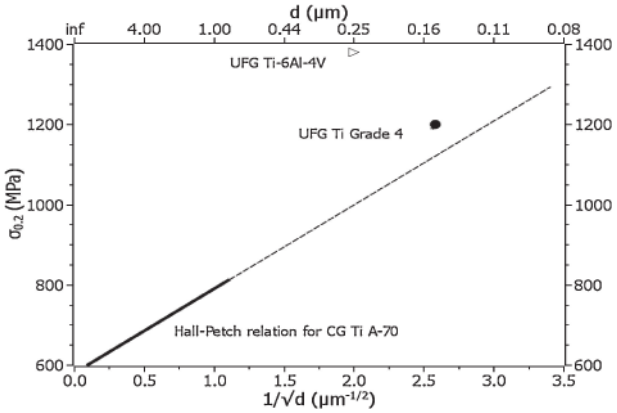

Fig. 9 The H–P relation for Ti, A-70[33] and data on the yield stresses of UFG Ti[14] and T–6%Al–4%V alloy.[38]

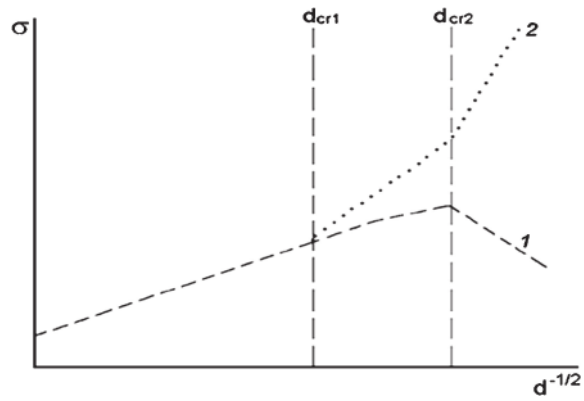

Fig. 10 Two types of the H–P slopes within different characteristic length scales.

From the available data it is seen that the σ_y values for the CG quenched alloys are close to the results for the Al–3% Mg alloy. However, for the UFG states in the 1570 and 7475 alloys with a grain size of 100–130 nm the value σ_y is considerably higher than calculated from the H–P relation for these grain sizes.

The H–P plot for Armco-Fe and commercially pure (CP) Ti (A-70, similar to Grade 4) are given in Figs. 8 and 9 correspondingly.[35–37] Here one can also see experimental data for several UFG materials produced by SPD. In case of CP Ti, the data are presented for HPT-processed UFG Ti–6%Al–4%V,[38] and also for UFG Ti, Grade 4 processed by ECAP and further thermomechanical treatment.[14] For CP Ti it is seen that in UFG state the σ_y values are higher than could be predicted by the H–P relation for the given grain sizes. Especially considerable excess of σ_y value is observed for the UFG alloy. For UFG Fe, the data on tensile mechanical tests are presented only by Ivanisenko *et al.*,[39] but there is evidence on microhardness H_v demonstrated in Fig. 9 using the ratio $\sigma_y = H_v/3$. The data for HPT-processed UFG steels 20 and 45 with 0.2 and 0.45%C content, respectively, are also presented here.[15,40] As in the case with Ti, there can be observed considerable excess of experimental σ_y values (especially, for steel 20) over the values predicted from the H–P relation.

Thus, the new phenomena of super-strength of nano-structured metals and alloys produced by SPD can be observed for various materials. Let us discuss the nature of the phenomena in details.

3.3 The origin of super-strength phenomena

As was pointed out above, in recent years the H–P behaviour in the range of ultrafine grain sizes became an object for numerous experimental and theoretical studies. However, for nano-sized grains (20–50 nm) this relation is typically reported to be violated so that the H–P plot deviates from linear dependence to lower stress values and its slope k_y often becomes negative (Fig. 10, curve 1). In the present work the examples reflecting the "positive" slope of the H–P relation are demonstrated (Fig. 10, curve 2).

Recently, on the basis of the experimental studies of materials obtained by vacuum depositions,[42] Firstov *et al.*[43] reported such "positive" slope of the H–P relation, where for the grain size range $d_{cr2} < d < d_{cr1}$ the exponent of d in eq. (1) was reported to vary from $-1/2$ to -1, and for $d < d_{cr1}$ the exponent of d is equal to -3.[43]

As was shown above in this work, positive slope of the H–P relation may be observed for SPD-processed metals as well. Though it is presently difficult to speak in terms of definite values for the exponent of d in eq. (1) due to a variety of grain boundaries in UFG metals and alloys, presently, however, it is possible that the presence of two characteristic grain size values is also valid for nano-structured SPD materials. Indeed, as has been already pointed out, the presence of non-equilibrium grain boundaries with dislocation arrays is typical for the majority of SPD materials, but definite GB structure is related to SPD processing regimes. It is known that GB influence on mechanical properties becomes considerable when the grain size is below 500–1000 nm. When the grain size decreases down to 100 nm and less a significant contribution of grain boundary segregations can be produced to the overall strength. Recently this question was especially addressed in Ref. 9) where it was shown that the high strength of UFG Al alloys is directly related to the formation of Mg segregations at grain boundaries revealed in the alloys by 3D APT technique.[9,12,44] In UFG materials deformation takes place

by dislocations generated at grain boundaries and moving through a grain to be captured by an opposite grain boundary. In this case the rate-controlling mechanism is "dislocation-grain boundary" interaction. Elevated concentration of solutes in grain boundaries can suppress emission of dislocations from such boundaries due to solute drag. As a result, the characteristic length and, correspondingly, activation volume of the deformation process will be reduced and a stress needed to emit a dislocation increases. This point is in good agreement with the recent experimental data.

Combination of a grain size strengthening with other strengthening mechanisms like precipitation or dislocation hardening can also lead to superstrength of UFG alloys. However, it seems that for metals and alloys subjected to SPD processing their contribution to total strength is essentially less than the influence of GB structures.[27)]

4. Conclusion

The conducted investigations testify to the fact that yield stress of UFG metals and alloys produced by SPD may be considerably higher than it is predicted by the H–P relation for their grain size range. The observed positive slope in H–P relation provides appearance of superstrength of these materials and this is associated with their grain boundaries structures, first of all with their non-equilibrium state and grain boundary segregations. Therefore, the design of grain boundaries in UFG materials produced by SPD techniques is quite important for the achievement of high strength in nanomaterials. Besides, it is topical for the ongoing research to study the role of intragranular nanostructural elements–nanotwins, nanoparticles, which can lead to additional strengthening of the materials.

Acknowledgements

This project was partially supported by the Russian Federal Ministry for Education and Science (RZV Contract No. 14.B25.31.0017). The author is very much grateful to Dr. N. A. Enikeev (Ufa, Russia) and Prof. T. G. Langdon (UK, USA) for useful discussions and several figures from our earlier publications indicated in the text as well as to colleagues from the NanoSPD community for the cooperation and publishing joint works, as cited in the reference section.

REFERENCES

1) E. O. Hall: Proc. Phys. Soc. Lond. Sect. B **64** (1951) 747.
2) N. J. Petch: J. Iron Steel Inst. **174** (1953) 25.
3) R. Z. Valiev: Nature Mater. **3** (2004) 511–516.
4) R. Z. Valiev, Y. Estrin, Z. Horita, T. G. Langdon, Z. Horita, M. J. Zehetbauer and Y. T. Zhu: JOM **58** (2006) 33.
5) C. Pande and K. Cooper: Prog. Mater. Sci. **54** (2009) 689.
6) C. Koch, I. Ovid'ko, S. Seal and S. Veprek: *Structural Nanocrystalline Materials: Fundamentals and Applications*, (Cambridge University Press, 2007).
7) F. Louchet, J. Weiss and T. Richeton: Phys. Rev. Lett. **97** (2006) 075504.
8) M. Kato, T. Fujii and S. Onaka: Mater. Trans. **49** (2008) 1278–1283.
9) R. Z. Valiev, N. A. Enikeev, M. Yu. Murashkin, V. U. Kazykhanov and X. Sauvage: Scr. Mater. **63** (2010) 949.
10) R. Z. Valiev, N. A. Enikeev and T. G. Langdon: Kovove Mater. **49** (2011) 1–9.
11) R. Z. Valiev, I. V. Alexandrov, N. A. Enikeev, M. Yu. Murashkin and I. P. Semenova: Rev. Adv. Mater. Sci. **25** (2010) 1–10.
12) P. V. Liddicoat, X. Z. Liao, Y. Zhao, Y. Zhu, M. Y. Murashkin, E. J. Lavernia, R. Z. Valiev and S. P. Ringer: Nat. Commun. (2010). doi:10.1038/ncomms1062.
13) R. Z. Valiev and T. G. Langdon: Adv. Eng. Mater. **12** (2010) 677.
14) I. Semenova, G. Salimgareeva, G. Da Costa, W. Lefebvre and R. Valiev: Adv. Eng. Mater. **12** (2010) 803–807.
15) M. V. Karavaeva, S. K. Kiseleva, M. M. Abramova, A. V. Ganeev, E. O. Protasova and R. Z. Valiev: Nanoengineering **10** (2013) 30–36.
16) M. P. Liu, H. J. Roven, M. Yu. Murashkin, R. Z. Valiev, A. Kilmametov and Z. Zhang: J. Mater. Sci. **48** (2013) 4758–4765.
17) R. Z. Valiev and T. G. Langdon: Prog. Mater. Sci. **51** (2006) 881.
18) H. P. Klug and L. E. Alexander: *X-ray Diffraction Procedures for Polycrystalline and Amorphous Materials*, New York, (John Wiley & Sons, 1974).
19) R. Z. Valiev, R. K. Islamgaliev and I. V. Alexandrov: Prog. Mater. Sci. **45** (2000) 103.
20) A. P. Zhilyaev and T. G. Langdon: Prog. Mater. Sci. **53** (2008) 893.
21) Y. Zhao, J. F. Bingert, X. Liao, B. Cui, K. Han, A. V. Sergueeva, A. K. Mukherjee, R. Z. Valiev, T. G. Langdon and Y. T. Zhu: Adv. Mater. **18** (2006) 2949.
22) Z. Horita, D. J. Smith, M. Furukawa, M. Nemoto, R. Z. Valiev and T. G. Langdon: J. Mater. Res. **11** (1996) 1880.
23) R. Z. Valiev and A. A. Nazarov: *Bulk Nanostructured Materials*, ed. by M. J. Zehetbauer and Y. Zhu, (T. Weinheim, Wiley-VCH Verlag GmbH & Co. KGaA, Germany, 2009) p. 21.
24) R. Z. Valiev, E. V. Kozlov, Yu. F. Ivanov, J. Lian, A. A. Nazarov and B. Baudelet: Acta Metall. Mater. **42** (1994) 2467.
25) G. Nurislamova, X. Sauvage, M. Murashkin, R. Islamgaliev and R. Valiev: Philos. Mag. Lett. **88** (2008) 459.
26) G. Sha, Y. B. Wang, X. Z. Liao, Z. C. Duan, S. P. Ringer and T. G. Langdon: Acta Mater. **57** (2009) 3123.
27) I. Sabirov, M. Yu. Murashkin and R. Z. Valiev: Mater. Sci. Eng. A **560** (2013) 1–24.
28) N. Krasilnikov, W. Lojkowski, Z. Pakiela and R. Valiev: Mater. Sci. Eng. A **397** (2005) 330.
29) A. W. Thompson: Acta Metall. **23** (1975) 1337.
30) C. Xiao, R. A. Mirshams, S. H. Whang and W. M. Yin: Mater. Sci. Eng. A **301** (2001) 35.
31) F. Ebrahimi, G. R. Bourne, M. S. Kelly and T. E. Matthews: Nanostr. Mater. **11** (1999) 343.
32) D. A. Hughes and N. Hansen: Acta Metall. **48** (2000) 2985.
33) N. Tsuji: Proc. NATO Science Series, Vol. **212**, Nanostructured Materials by High-Pressure Severe Plastic Deformation, ed. by Y. T. Zhu and V. Varyukhin, (Dordrecht, Springer Netherlands, 2006) pp. 227–234.
34) M. Furukawa, Z. Horita, M. Nemoto, R. Z. Valiev and T. G. Langdon: Philos. Mag. A **78** (1998) 203.
35) R. L. Jones and H. Conrad: Trans. Met. Soc. AIME **245** (1969) 779.
36) I. Charit and K. L. Murty: Trans. SMiRT **19** (2007) 1–6.
37) T. R. Malow and C. C. Koch: Metall. Mater. Trans. A **29** (1998) 2285.
38) A. V. Sergueeva, V. V. Stolyarov, R. Z. Valiev and A. K. Mukherjee: Mater. Sci. Eng. A **323** (2002) 318.
39) Yu. Ivanisenko, A. V. Sergueeva, A. Minkow, R. Z. Valiev and H.-J. Fecht: *Nanomaterials by Severe Plastic Deformation*, ed. by M. J. Zehetbauer and R. Z. Valiev, (Wiley-VCH, Weinheim, Germany, 2004) p. 453.
40) M. V. Chukin, N. V. Koptseva, R. Z. Valiev, I. L. Yakovleva, J. Zrnik and T. Covarik: Vestnik MGTU **1** (2008) 31.
41) R. Z. Valiev, Y. V. Ivanisenko, E. F. Rauch and B. Baudelet: Acta Mater. **44** (1996) 4705.
42) S. A. Firstov, T. G. Rogul, V. T. Marushko and V. A. Sagaydak: Vopr. Materialoved. (The Issues of Materials Science) **33** (2003) 201.
43) S. A. Firstov, T. G. Rogul and O. A. Shut: Funct. Mater. **16** (2009) 4.
44) X. Sauvage, G. Wilde, S. V. Divinski, Z. Horita and R. Z. Valiev: Mater. Sci. Eng. **540** (2012) 1–12.